ELSEVIER

Journal of Alloys and Compounds 293–295 (1999) 675–679

Journal of ALLOYS AND COMPOUNDS

Mg_2Ni-based hydrogen storage alloys for metal hydride electrodes

J. Chen*, P. Yao, D.H. Bradhurst, S.X. Dou, H.K. Liu

Institute for Superconducting & Electronic Materials, University of Wollongong, Wollongong, NSW 2522, Australia

Abstract

$Mg_{2-X}M_XNi$ (M=Ti, Ce; X=0, 0.1, 0.2) and $MgNi_{1-y}N_y$ (N=Mn, Co; y=0, 0.1, 0.2) were prepared by a powder metallurgical sintering technique. The effects of the element substitutions and the ball-milling of the alloy, with or without nickel powder, on the alloy properties were investigated by X-ray diffraction, transmission electron microscopy and the Malvern particle size analyser. Three types of alloys, un-ball-milled, ball-milled without nickel powders and ball-milled with the addition of nickel powders, were used as the active material of metal hydride electrodes. Electrochemical measurements show that ball-milling the alloy with or without nickel powders is an effective method for increasing the discharge capacity and cycle life of the alloy electrode because of the changed phase structure and surface behaviour.

Keywords: Mg_2Ni-based hydrogen storage alloys; Ball milling; Electrochemical properties

1. Introduction

Mg-based hydrogen storage alloys as the active materials of metal hydride electrodes have attracted attention because of their high theoretical capacities for hydrogen absorption/desorption [1]. Recently, the charge–discharge properties of Mg-based alloys at room temperature have been improved greatly by some research groups [2–5]. In particular, the partial substitution of Mg by Al or Mn from Mg_2Ni and the ball-milling of Mg_2Ni alloy with Ni powder were found to be very useful methods for improving the high discharge capacity. Kohno et al. [4] proposed that the long-time ball-milling could result in the fact that the size of crystal grains becomes smaller and the heterogeneous strain increases. Iwakura et al. [5] reported that the homogeneous amorphous microstructural characteristic is responsible for the improvement in charge–discharge properties. Although a high discharge capacity around 800 mAh/g was achieved, the capacity decay of the Mg-based alloy electrode is still serious, which makes it difficult to be used as the electrode material in practice.

To improve the characteristics of Mg-based hydrogen storage alloy, Mg and Ni from Mg_2Ni alloy were partially substituted by Ti or Ce and Mn or Co, respectively. Also, the technique of ball-milling in controlled conditions was used.

2. Experimental

Alloys of Mg_2Ni, $Mg_{2-X}M_XNi$ (M=Ti, Ce; X=0, 0.1, 0.2) and $MgNi_{1-y}N_y$ (N=Mn, Co; y=0, 0.1, 0.2) were prepared by a powder metallurgical sintering technique. The appropriate amounts of metal powders ($\leq$ 3 μm from Aldrich Chemical Company) with the purity of at least 99.7 wt.% were thoroughly mixed and pressed into pellets. The pellets were first sintered at 620°C for 10 h under argon atmosphere, then ground into powders which were sieved to control the particle size in the range between 36–46 μm. These powders were ball-milled in an argon atmosphere with control of the ball movement and temperature. In this work the powder, which was ball-milled the alloy with 10 wt.% nickel powder, is designated as BM-Ni-alloy. The powder ball-milled in the absence of nickel powder is designated as BM-alloy. Structure and phase identification of the alloy powders were investigated by X-ray diffraction (XRD) using Cu Kα radiation and transmission electron microscopy (TEM) using a JEOL 2000 FX. Particle size distribution and specific surface area of the alloys were examined using a Malvern particle analyser (PA).

The BM-Ni-alloy powders were mixed with 1.5% polyvinyl alcohol (PVA) solution, and then pasted into a nickel foam with a porosity of 95% (0.5×0.5 cm). For comparison, the BM-alloy powders, mixed with 10wt.% Ni powder, were also pasted as the same way. Both kinds of

*Corresponding author.

0925-8388/99/$ – see front matter
PII: S0925-8388(99)00429-6

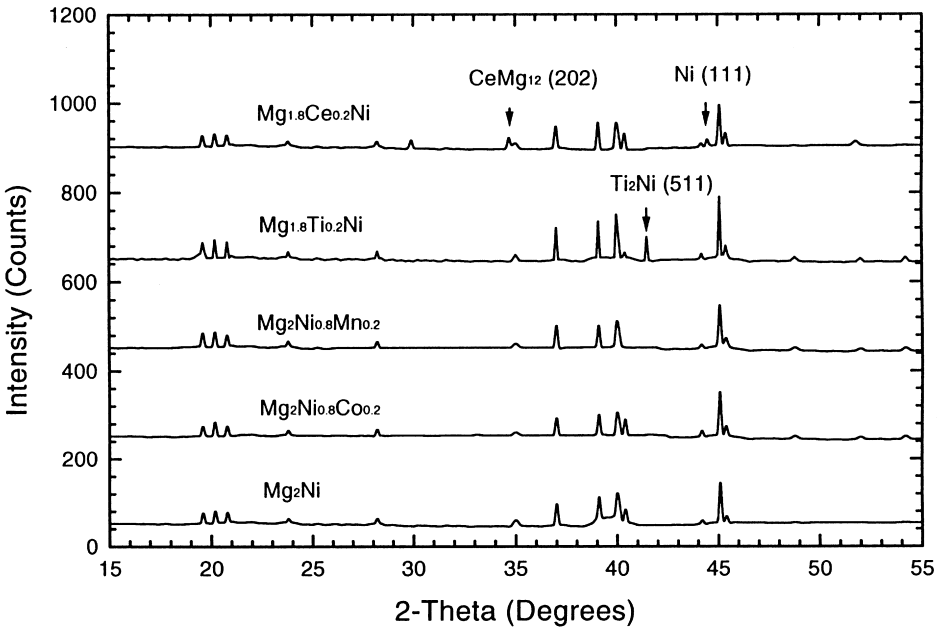

Fig. 1. X-ray diffraction profiles of $Mg_{1.8}M_{0.2}Ni$ (M=Ti, Ce) and $Mg_2Ni_{0.8}N_{0.2}$ (N=Mn, Co).

electrodes were then dried at 100°C under vacuum for 1 h before pressing at 900 kg cm^{-2}. Electrode properties were tested in a half-cell consisting of the MH working electrode, the $NiOOH/Ni(OH)_2$ counter electrode, a Hg/HgO reference electrode and 6 M KOH electrolyte. The electrodes were charged at a current density of 50 mA/g for 20 h, rested for half hour and then discharged at 50 mA/g to −600 mV versus the Hg/HgO electrode. When the capacity was calculated, only the weight of the hydrogen storage alloy was considered.

3. Results and discussion

Fig. 1 shows the XRD profiles of the Mg_2Ni, $Mg_{1.8}M_{0.2}Ni$ (M=Ti, Ce) and $MgNi_{0.8}N_{0.2}$ (N=Mn, Co). They exhibit similar patterns which could be indexed as a hexagonal structure. Additional peaks marked with arrows might be indexed to other phases such as Ti_2Ni in $Mg_{1.8}Ti_{0.2}Ni$, $CeMg_{12}$ and Ni in $Mg_{1.8}Ce_{0.2}Ni$. It is to be pointed out that the reasons why the elements of Ti, Ce, Mn and Co to be selected are: (1) Ti: good hydrogen storage and passive oxide (TiO_2); (2) Ce: good hydrogen storage and is a protective surface film (CeO_2); (3) Mn: destabilises ΔH and is a catalyst for hydrogen oxidation; (4) Co: destabilises ΔH, is resistant to oxidation, is a catalyst for hydrogen oxidation and reduces volume expansion which is observed in AB_5 system alloys [6].

The effects of partial substitutions of Mg and Ni in Mg_2Ni on the electrode capacities are summarised in Table 1. Both Ti and Ce substitution for Mg not only increases the discharge capacity of the alloy electrode, but also improves the cycle life. The partial substitution of Mn or Co for Ni increases the capacity and has little effect on the cycle life.

Fig. 2 shows the XRD patterns of (a) BM-$Mg_{1.8}Ti_{0.2}Ni$ and (b) BM-Ni–$Mg_{1.8}Ti_{0.2}Ni$. For BM-$Mg_{1.8}Ti_{0.2}Ni$, the characteristic peaks of the Mg_2Ni phase decreased in intensity and broadened, indicating that there was a phase transformation from polycrystalline to amorphous or

Table 1
Discharge capacity and cycle life of the Mg-based alloy electrodes

Alloy composition	The highest capacity (mAh/g)	Cycle life (to zero capacity)
Mg_2Ni	55	7
$Mg_{1.9}Ti_{0.1}Ni$	88	16
$Mg_{1.8}Ti_{0.2}Ni$	90	19
$Mg_{1.9}Ce_{0.1}Ni$	83	14
$Mg_{1.8}Ce_{0.2}Ni$	85	17
$Mg_2Ni_{0.9}Mn_{0.1}$	78	8
$Mg_2Ni_{0.8}Mn_{0.2}$	74	7
$Mg_2Ni_{0.9}Co_{0.1}$	76	9
$Mg_2Ni_{0.8}Co_{0.2}$	70	10

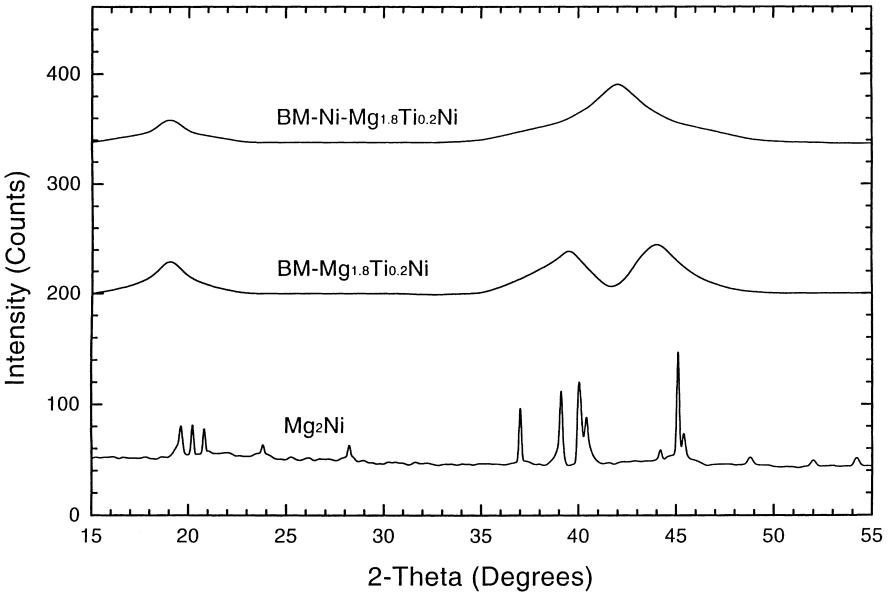

Fig. 2. X-ray diffraction patterns of (a): ball-milled and (b): nickel-ball-milled $Mg_{1.8}Ti_{0.2}Ni$ alloys.

nanocrystalline state. For BM-Ni–$Mg_{1.8}Ti_{0.2}Ni$, a more broaden peak was detected, and no peaks identified as metallic Ni were observed. Similar results were also investigated by Iwakuau et al. [5]. This illustrates that a high degree of dispersion of nickel in the alloy and might form a nonstoichiometric structure. In both conditions the characteristic peaks of the $Mg_{0.8}Ti_{0.2}Ni$ phase decreased in intensity and broadened, and this is normally considered as the amorphous structure. XRD peak broadening is due to the very fine grain size and is characteristic of typical structures for ball-milling. Similar phase transformation was also observed in the other alloys and not shown in this paper.

A TEM analysis of $Mg_{1.8}Ti_{0.2}Ni$ alloy before ball-milling [Fig. 3a] gives the relative markable features coming from the multicrystals and also demonstrates that some large crystal particles remain. The halo patterns centred in Figs. 3b and c reveal the strong incoherent scattering of the beam electrons in the amorphous-like state of $Mg_{1.8}Ti_{0.2}Ni$ after ball-milling, and the diffraction rings show that some nanocrystal grains coexist with the amorphous. Compared with Fig. 3b, the broadening of the rings in Fig. 3c contribute to the smaller size of the crystal grains.

The effects of the ball-milling on the particle size distributions and specific surface areas of the $Mg_{0.8}Ti_{0.2}Ni$ are summarised in Table 2. It can be seen that the ball-milling results in a gradual reduction in the lamella spacing from 36–46 μm for the alloy powder before ball-milling to 0.08–1.5 μm for the BM-$Mg_{1.8}Ti_{0.2}Ni$ and 0.07–1.4 μm for the BM-Ni–$Mg_{1.8}Ti_{0.2}Ni$. Also it is obvious that the specific surface area was greatly increased after the ball-milling. The ball-milling is a means of prolonged time of collision between the balls and the alloy particles, and subsequently the alloy particles are fractured and inter-diffusion takes place resulting in the large increase of specific surface area. It is thought that the ball-milled mixtures contain many defects such as dislocations, grain boundaries and microvoids which are mainly formed during the ball-milling process. These defects may trap hydrogen during the diffusion process so that the energy level of these sites is lower than that of the normal sites of the lattice [7]. As a result, the alloys after ball-milling will convey obvious advantages for hydrogen absorption/desorption (charge/discharge).

The effects of the ball-milling (with or without the addition of nickel powder) on the electrode properties of Mg_2Ni, $Mg_{1.8}M_{0.2}Ni$ (M=Ti, Ce) and $Mg_2Ni_{0.8}N_{0.2}$ (N= Mn, Co) are listed in Table 3. Compared with the data listed in Table 1, it can be clearly seen that: (1) the discharge capacities of the studied Mg-based alloy electrodes are greatly improved by the ball-milling; (2) the capacity of each alloy ball-milled with nickel powder is higher than that of the alloy in the absence of nickel powder; (3) the cycle life of the electrode is increased after ball-milling with the addition of nickel powder; and (4) the cycle life of the electrode is also increased by the partial substitutions of Mg by Ti and Ni by Co.

Discharge curves of the $Mg_{1.8}Ti_{0.2}Ni$ electrodes at a current density of 50 mA/g in the third cycle are shown in Fig. 4. The curves show that the discharge performance of the $Mg_{1.8}Ti_{0.2}Ni$ alloy electrode is greatly improved by the ball-milling. No discharge plateau is detected for the alloy without ball-milling, but a plateau of discharge potential is observed around −0.84 V versus Hg/HgO electrode for the alloy after ball-milling (with or without nickel powder).

To analyse the capacity decay, the active materials of the BM-Ni–Mg_2Ni electrode (at the 28th cycle) and the

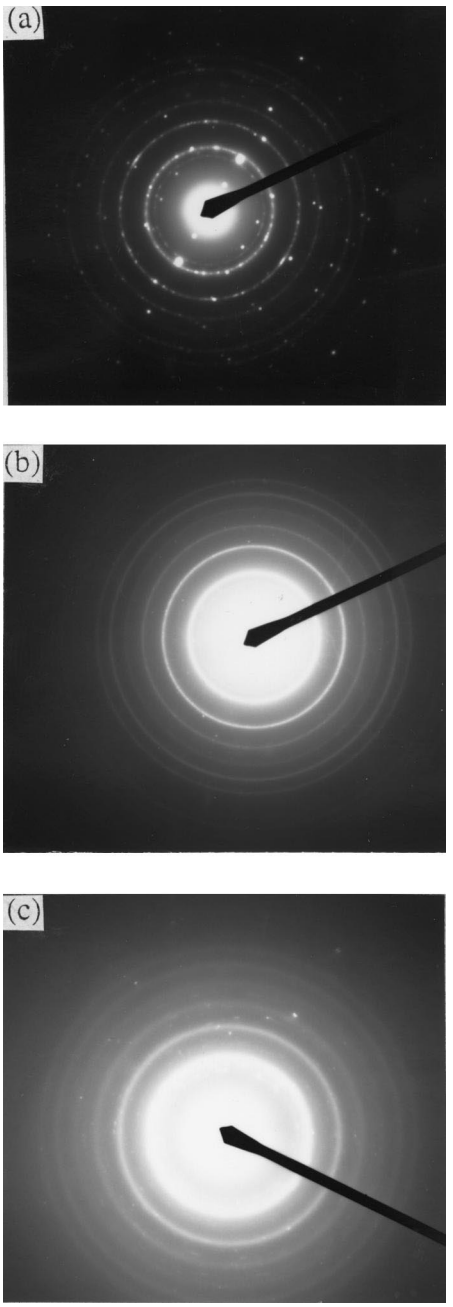

Fig. 3. Transmission electron microscopy images for (a): un-ball-milled; (b): ball-milled and (c): nickel-ball-milled $Mg_{1.8}Ti_{0.2}Ni$ alloys.

Table 2
Particle size distribution (PSD) and specific surface area (SSA) for $Mg_{0.8}Ti_{0.2}Ni$ alloys

Alloy samples	PSD (μm)	SSA ($m^2\ g^{-1}$)
$Mg_{1.8}Ti_{0.2}Ni$	36–46	0.2
BM-$Mg_{1.8}Ti_{0.2}Ni$	0.08–1.5	12.8
BM-Ni–$Mg_{1.8}Ti_{0.2}Ni$	0.07–1.4	14.6

Table 3
Discharge capacity and cycle life of the ball-milled (BM) and nickel ball-milled (BM-Ni) Mg-based alloy electrodes

Alloy	$C_{max.}$ (mAh/g)	Cycle No. (to 100 mAh/g)
BM-Mg_2Ni	420	12
BM-Ni–Mg_2Ni	680	28
BM-$Mg_{1.8}Ti_{0.2}Ni$	490	20
BM-Ni–$Mg_{1.8}Ti_{0.2}Ni$	720	42
BM-$Mg_{1.8}Ce_{0.2}Ni$	414	17
BM-Ni–$Mg_{1.8}Ce_{0.2}Ni$	658	31
BM-$Mg_2Ni_{0.8}Mn_{0.2}$	580	15
BM-Ni–$Mg_2Ni_{0.8}Mn_{0.2}$	756	32
BM-$Mg_2Ni_{0.8}Co_{0.2}$	470	16
BM-Ni–$Mg_2Ni_{0.8}Co_{0.2}$	710	38

BM-Ni–$Mg_{1.8}Ti_{0.2}Ni$ electrode (at the 42nd cycle) were analysed by XRD, as shown in Fig. 5. It can be seen that $Mg(OH)_2$ is formed not only in the BM-Ni–Mg_2Ni but also in the BM-Ni–$Mg_{1.8}Ti_{0.2}Ni$. However, the peak intensity of this oxide is much stronger in the former one than that in the latter one. The serious oxidation of these alloys is because of the more active reaction in the alkaline electrolyte. Also the characteristic peak of TiO_2 is detected in the BM-Ni–$Mg_{1.8}Ti_{0.2}Ni$. The formation of TiO_2 could prevent the alloy from being oxidised to some extent, and therefore shows the longer cycle life observed in Table 3.

4. Conclusions

Both Ti and Ce are effective as a partial substitute for Mg from Mg_2Ni in improving discharge capacity and cycle life of the alloy as the anode active material of a nickel–metal hydride cell. Partial substitution of Ni by Mn or Co from Mg_2Ni increases the discharge capacity and has little effect on the cycle life. Ball-milling the alloy with or without nickel powder is an effective method of improving the electrode properties of Mg-based alloys because of the changed amorphous structure and increased specific surface area. The electrode containing the nickel ball-milled $Mg_{1.8}Ti_{0.2}Ni$ alloy gives a discharge capacity of 720 mAh/g (at the discharge current density of 50 mA/g) and over 42 cycles (to specific capacity of 100 mAh/g) indicating that the kinetics of hydrogen absorption/desorption (charge/discharge) for this alloy are greatly improved by the addition of Ti and the ball-milling process.

Acknowledgements

Financial support by the Department of Employment, Education and Training (DEET) is gratefully acknowledged.

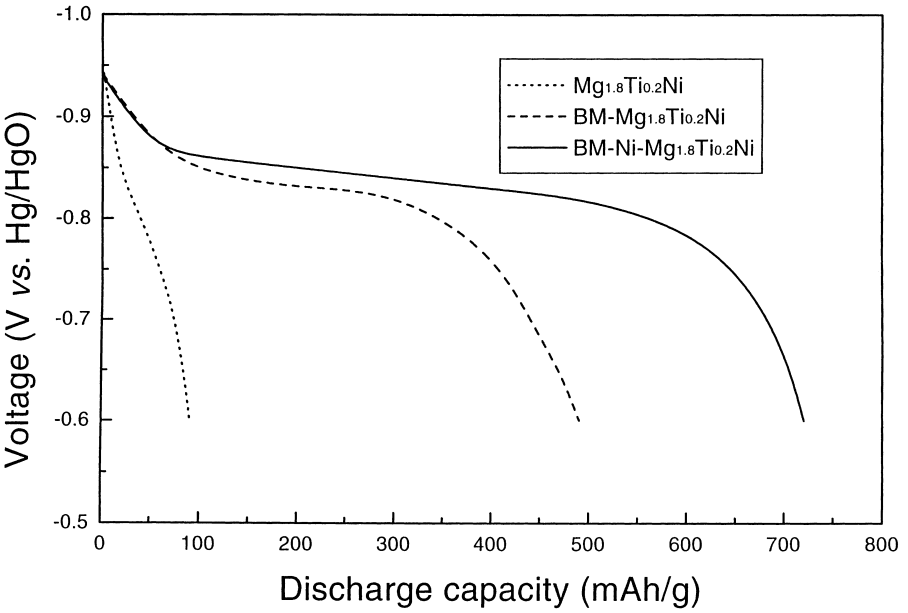

Fig. 4. Discharge curves (the third cycle) of the un-ball-milled, ball-milled and nickel-ball-milled $Mg_{1.8}Ti_{0.2}Ni$ alloys.

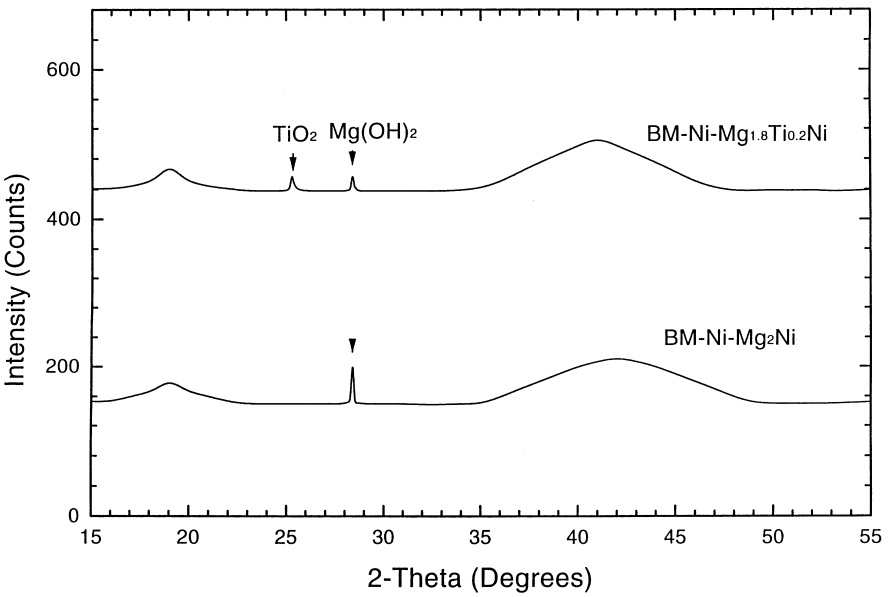

Fig. 5. X-ray diffraction patterns of (a): the nickel-ball-milled Mg_2Ni at the 28th cycle; and (b): the nickel-ball-milled $Mg_{1.8}Ti_{0.2}Ni$ at the 42nd cycle.

References

[1] C. Iwakura, S. Hazui, H. Inoue, Electrochemica Acta 41 (1996) 471.
[2] Y.Q. Lei, Y.M. Wu, Q.M. Yang, J. Wu, Q.D. Wang, Z. Phys. Chem. 183 (1993) 379.
[3] N. Cui, B. Luan, H.K. Liu, H.J. Zhao, S.X. Dou, J. Power Sources 55 (1995) 263.
[4] T. Kohno, M. Kanda, J. Electrochem. Soc. 144 (1997) 2384.
[5] S. Nohara, N. Fujita, S. Zhang, H. Inoue, C. Iwakura, J. Alloys Comp. 267 (1998) 76.
[6] J.J.G. Willems, Philips J. Research 39 Supplement (1984) 1.
[7] J. Senegas, M.Y. Song, M. Pezat, B. Darriet, J. Less-Common Met. 129 (1987) 317.